

Percentage fat fraction in magnetic resonance imaging: Upgrading the osteoporosis-detecting parameter

Rong Chang

Honghui Hospital

Xiaowen Ma

Honghui Hospital

Yonghong Jiang

Honghui Hospital

Dageng Huang

Honghui Hospital

Xiujin Chen

Honghui Hospital

Ming Zhang

First Affiliated Hospital, Medical College Xi'an Jiaotong University

Dingjun Hao (✉ cr4512015105@163.com)

Honghui Hospital

Research article

Keywords: Osteoporosis, bone mineral density, magnetic resonance imaging, fat fraction; m-Dixon-Quant MRI

Posted Date: August 28th, 2019

DOI: <https://doi.org/10.21203/rs.2.13669/v1>

License: © ⓘ This work is licensed under a Creative Commons Attribution 4.0 International License.

[Read Full License](#)

Version of Record: A version of this preprint was published at BMC Medical Imaging on March 17th, 2020. See the published version at <https://doi.org/10.1186/s12880-020-00423-0>.

Abstract

Background: Osteoporosis (OP) is a common metabolic bone disorder and orthopedic imaging approaches were commonly used with some limitations. The aim of this study was to explore the diagnostic value of magnetic resonance 1-H MRS and m-Dixon-Quant in the evaluation of osteoporosis

Methods: We enrolled 76 subjects and used a quantitative computed tomography (QCT) technique to determine the subjects' bone mineral density (BMD). Those with a BMD >120 mg/cm³ were categorized as the normal control; those with a BMD ranging from 80–120 mg/cm³ were classified as having osteopenia; and those with a BMD <80 mg/cm³ were diagnosed as having OP. The following parameters were recorded for each patient: sex, age, body height, body weight, waist circumference, and hip circumference. Simultaneously, the FF% values from 1-H MRS examinations and m-Dixon-Quant scans were acquired.

Results: In both 1-H MRS and m-Dixon-Quant MRI, the FF% exhibited a negative correlation with BMD. Among the different groups, the OP patients had a significantly higher FF% compared to healthy subjects. In addition, the FF% in the m-Dixon scans exhibited a positive correlation with age, while BMD showed a negative linear relationship with age. Further, females had a higher FF% compared to males, and body height was correlated with BMD but not with FF%.

Conclusions: MRI investigations (especially FF% in the m-Dixon-Quant imaging system) are useful in OP assessments. Also, parameters such as sex, age, and height are important factors for predicting and diagnosing OP.

Background

Osteoporosis (OP) is a common metabolic bone disorder that affects more than 200 million people worldwide¹, which was with clinical features of reduced bone density and increased bone fragility. OP patients showed a high susceptibility to fracture, especially vertebral compression fracture (VCF, or benign compression fracture)². In VCF cases, the bone mass gradually reduces and the microarchitectural deterioration of bone tissue accumulates; even slightly force is strong enough to cause a fracture³.

The diagnosis of OP is largely based on following orthopedic imaging approaches⁴. First, since the 1990s, the World Health Organization's (WHO) operational definition of OP, as based on the bone mineral density (BMD) (determined by dual-energy X-ray absorptiometry [DXA]), has been used globally⁵. DXA provides mineral content and also help to diagnose OP in a patient with a lower BMD T-score (mean BMD value - 2.5) in a population of 30-year-old individuals of the same sex and race. It has been recognized that the low areal BMD is strongly associated with an increased risk of fracture in OP patients⁶, and the fracture risk nearly doubles for every standard deviation decrease in BMD⁷. To date, BMD is still the golden quantitative parameters for OP diagnosis, which is a particularly strong predictor of future

osteoporotic fractures. However, BMD assessments using DXA have several known limitations. Many patients were misclassified as having false-negative diagnoses and subsequently received delayed treatments⁸. BMD changes quite slowly⁹, and there is controversy surrounding the antifracture effects of OP drugs and the corresponding response in BMD values. Moreover, DXA is generally not used in scans of fractured vertebrae. Vertebral fractures are generally more common in compression fractures, which easily affect the results of bone density measurement. In addition, ionizing radiation may cause radiation sickness which is a systemic reaction of the body. Pathological changes occur in almost all organs and systems, but the changes in the nervous system, hematopoietic organs and digestive system are most obvious. The second available tool that is used to determine a diagnosis of OP is computed tomography (CT), which also uses ionizing radiation; however, CT is limited in differentiating healed from non-healed fractures. Another widely used method of OP detection is use of an ultrasound bone densitometer¹⁰; however, this approach was mainly validated only for calcaneus, also used for radius. Besides, US spine densitometry is in the research stage.

Therefore, patients urgently need novel tools to diagnose OP and assess fracture risk, as well as to monitor response to therapies. Magnetic resonance imaging (MRI) is a useful, non-invasive tool that can be used to acquire in vivo images of the living body without the need for X-ray ionizing radiation. MR spectroscopy (MRS) is one of the most useful approaches in MRI. It can differentiate healed from non-healed fractures in the human body without the need for radiation¹¹. Previous studies of the lumbar spine have indicated that bone density has a negative relationship with bone marrow fat content. The 1H MRS method has been used for the quantitative assessment and differential diagnosis of brain tumors¹². It is the only noninvasive method that can provide information on the biochemical profile of patient tissues in vivo¹³. Conversely, the m-Dixon-Quant technique is a novel update of MRI¹⁴. It arbitrarily selects echoes in the signal-acquisition process, thus effectively shortening the TE time. The m-Dixon-Quant technique combines parallel acquisition technologies such as SENSE and dS-SENSE to enhance the imaging speed, and it largely improves the resolution when the noise ratio is minimized. This technique was found to be effective at calculating lipid content in vivo.

One known mechanism of spinal OP is that the adipogenic differentiation of mesenchymal stem cells (MSCs) is upregulated when compared to osteogenic differentiation in the spinal marrow. When this balance is broken, the fat fraction increases, which can be reflected in the MRS and m-Dixon-Quant imaging system. Based on this, we hypothesized that the fat fraction percentage (FF%) could be used to predict and diagnose OP. In this study, in order to explore the diagnostic value of magnetic resonance 1-H MRS and m-Dixon-Quant in the evaluation of osteoporosis, we combined results of both methods and proposed a novel diagnostic strategy that could be valuable in providing a clinically quantitative analysis of OP.

Methods

Patients

This study was reviewed and approved by the ethics committee of Hong Hui Hospital, Xi'an Jiaotong University, and performed between May 2016 and October 2017. We enrolled 76 subjects (age: 59.18 ± 9.22 years; 46 males and 30 females; males, 59.17 ± 9.06 years old and females, 59.20 ± 9.61 years old) and divided them into three groups according to their BMD measurement: healthy controls (18 cases), osteopenia (30 cases), and OP (28 cases). The exclusion criteria were as follows: (1) the presence of metabolic bone diseases; (2) those who had a history of spinal surgery; and (3) those who received drug therapy for OP. The following parameters were recorded for each patient: sex, age, body height, body weight, waist circumference, and hip circumference. All patients signed informed consent and agreed to participate in the survey. The study was also approved by the hospital ethics committee of our hospital.

BMD Measurements

The quantitative CT (QCT) technique was used for BMD measurements. All recruited patients underwent QCT scanning of the anterior–posterior lumbar spine (L2–L4) and their BMD values were expressed in mg/cm^3 . PHILIPS 16-slice spiral CT reconstruction was applied to obtain QCT values.

According to the American College of Radiology (ACR) Guidelines for Quantitative CT (QCT), subjects were divided into three categories based on their BMD results: those with a BMD $>120 \text{ mg}/\text{cm}^3$ were designated as the normal control, those with a BMD from $80\text{--}120 \text{ mg}/\text{cm}^3$ were diagnosed as having osteopenia, and those with a BMD $<80 \text{ mg}/\text{cm}^3$ were diagnosed as having OP.

The BMD values of the L2, L3, and L4 vertebrae were obtained, and the average BMD was calculated using the mean value of L2, L3, and L4. An OP or osteopenia diagnosis was primarily determined according to the average BMD value (henceforth abbreviated as BMD).

1-H MRS examination

For all subjects, routine MR scans and 1-H MRS scans were performed when available. In all, 52 cases received the MR scan. The 1.5T PHILIPS superconducting MR machine was used for spectral acquisition. Through conventional MRI plain scanning, as well as sagittal and transverse scanning, the following indexes were set: T2WI/TSE TR 2500, TE 100, two acquisitions, FOV $160 \times 302 \times 57$ mm, layer thickness 4 mm, spacing 0.8 mm, matrix 180×237 ; and T1WI/TSE TR 400, TE 8, FOV $160 \times 299 \times 57$ mm, layer thickness 4 mm, spacing 0.8 mm, matrix 160×214 . The 1H MRS scan used a single element Point Resolved Spectroscopy (PRESS) sequences for the sagittal and transverse scans. The MRS scan parameters were as follows: TR 2,000 ms; TE 42 ms; wave width 1,000 ms; excitation frequency 120 times; voxel $15 \text{ mm} \times 15 \text{ mm} \times 12 \text{ mm}$. The area was reproducible and easy to operate. Previous studies have shown that the lower the bone fat content of the vertebral body, the lower the fat content, the higher the fat content. Thereby, the middle vertebral body was taken as the representative. We recorded the water peak of the L3 vertebral body displacement around 4.70 ppm and the fat peak between 1.30 and 0.90 ppm.

The subjects' FF% values were calculated using the formula: $FF\% = I_{fat} / (I_{water} + I_{fat}) * 100\%$, where I_{water} or I_{fat} represented the peak of fat or water in the examined substance. This parameter refers to the relative fat signal strength amplitude in relation to the total amplitude (water + fat). After scanning with 1H MRS and m-Dixon-Quant sequences, post-processing software of PHILIPS MR machine automatically calculated I_{water} or I_{fat} values.

m-Dixon-Quant scanning

The 1.5T PHILIPS superconducting MR machine (Philips Medical Systems, Best, Netherlands) was also used to capture the m-Dixon-Quant images at the same time. The conventional settings were identical to the 1H MRS protocols. For the MRI m-Dixon-Quant 3D scan, six phase diagrams were acquired toward three lumbar vertebrae. The medullary cavity was in the central region of the vertebral body, which avoiding the cortical bone at the edge of the vertebral body, and drawing a rectangle of 15 mm*15 mm*12 mm at the center of the L3 vertebral body as the region of interest. Then, we measured on the fat map made by 1 m-Dixon-Quant. The scanning parameters were as follows: TR 7 ms; multi-echo; echo chain 6; NSA 2, flip angle 5°; FOV 300*369*120; voxel 2*2*4; layer thickness 6 mm; spacing 3 mm; matrix 152*184*60; scan mode 3D; and scan time 51 seconds. The FF% value was directly reported by the PHILIPS superconducting MR machine (with the Philips 3.0tx superconducting MRI scanner software). The target area of the MRI analysis was the same as the area of the BMD measurement point.

Statistical analysis

All results were presented as the mean \pm standard deviation (SD). The relationship between pairs of variables was assessed using the linear correlation analysis (Pearson's R coefficient). Differences between groups were assessed with one-way ANOVA and the difference between males and females was compared using unpaired *t*-tests. *P*-values <0.05 were considered statistically significant.

Results

Fat fraction is negatively correlated with bone density

First, we used the parameter FF% in both 1H MRS and m-Dixon-Quant methods, and the results consistently showed that the average BMD had a negative relationship with FF% level. As shown in Figure 1A, the 1H MRS data included 52 cases and a significant non-zero slope was found ($Y = -0.1906 * X + 75.08$; Pearson's $R^2 = 0.1046$; $P = 0.0194$). Similarly, data derived from m-Dixon-Quant imaging included 76 cases, with a highly significantly negative correlation between the average bone density and FF% ($Y = -0.1201 * X + 69.15$; Pearson's $R^2 = 0.2200$; $P < 0.001$). We divided the patients into three groups (healthy

controls, osteopenia, and OP), and a consistent conclusion could be drawn (Figure 1B). The FF% value was significantly higher in the OP group when compared to the controls (m-Dixon-Quant method: FF% = 51.25 ± 7.38 in the control group; 54.70 ± 8.30 in the osteopenia group; and 62.53 ± 5.02 in the OP group; OP versus control, $P < 0.05$). Two individuals in the OP and healthy groups were presented in Figure 2. The lipid peaks of the L2 vertebral body in OP patients was significantly increased when compared to healthy controls (Figures 2A and 2B), as shown in the 1H MRS quantitative analysis; the same trend was observed for the L3 vertebral body during the m-Dixon-Quant analysis (Figures 2C and 2D). These results suggest that both 1H MRS and m-Dixon-Quant imaging could measure bone marrow fat content, and this had high clinical value in the diagnosis of OP.

Sex and age correlate with BMD and FF% changes

In addition to FF%, we analyzed other variables like the sex, age, height, and weight of each patient to probe for more references that might aid in reaching a diagnosis. As expected, age is a useful reference parameter, which largely determined BMD and FF levels (Figure 3A). The FF% from the m-Dixon scan exhibited a positive correlation with age ($F_{1,74} = 16.35$, $P < 0.0001$, $Y = 0.3807 * X + 34.97$, Pearson's $R^2 = 0.1810$), while BMD showed a negative linear relationship ($F_{1,74} = 42.77$, $P < 0.0001$, $Y = -2.216 * X + 227.6$, Pearson's $R^2 = 0.3727$). This is consistent with the widely agreed upon knowledge that older adults have a greater risk for developing OP. Further, we found that females had a higher FF% level compared to males (t -test; $P < 0.01$) (Figure 3B). Interestingly, body height was found to be positively correlated with BMD ($F_{1,72} = 4.747$, $P < 0.05$, $Y = 0.9652 * X - 63.63$, Pearson's $R^2 = 0.06185$), but not FF% ($P = 0.064$) (Figure 3C). This finding was reasonable, insofar as a taller body implied a stronger bone density, but the correlation was much lower than it was for parameters such as sex and age. Finally, we did not observe any influence of body weight, waist circumference, and hip circumference on either BMD or FF%. Together, sex and age correlate with BMD and FF% changes, and these parameters may help to diagnose and predict OP when combined with 1H MRS or m-Dixon techniques.

Discussion

In this study, we applied 1H MRS and m-Dixon-Quant 3D scanning to aid in diagnosing OP; we also proposed a novel reference insofar as FF% may reflect the BMD value. In combination with the sex, age, and height of each patient, MRI can be a useful means for detecting the early warnings of OP development.

Compared with QCT, MRI has the distinct advantage of being nonradiative¹⁵. In this way, if ample economic resources are available, MRI can be repeatedly performed for those patients with similar phenotypes of OP, and this may be especially true for older women. Moreover, our results hold clinical value, not only in terms of being able to make orthopedic diagnoses, but they can also be used in other clinical divisions; specifically, some MRI scanning without a strong purpose of bone density detection may unexpectedly discover a potential OP.

Thus far, MRI is the only non-invasive method to provide quantitative analysis of tissue metabolism, biochemical environments, and compounds in living organisms. When a pathological change occurs, the metabolic abnormality of the tissue usually precipitates structural changes. Therefore, MRI can detect diseases early on when compared to the QCT technology¹⁶. Based on these principles, many researchers have carried out similar studies to show the relationship between BMD and other MRI indexes in the evaluation of OP. Most studies demonstrated findings that were consistent with those of our work. As early as 2000, researchers observed the whale vertebrae and human distal tibia through QCT and MRI where they noticed that MRI data can be used to measure bone density and cross-sectional geometry¹⁷. Later, fat–water MRI signal intensities were reported to be significantly correlated with BMD from QCT in a human patella experiment¹⁸. An estimation of trabecular bone parameters in children revealed correlations of >0.7 between the parameters obtained from MRI and the values obtained from high-resolution HR-QCT¹⁹. A cadaver bone histology study also found a statistically significant inverse association between marrow fat (determined by MRI) and BMD (determined by DXA)²⁰. Moreover, the apparent diffusion coefficient values of vertebral bone marrow acquired by the MR diffusion-weighted imaging system were reported to be positively correlated with BMD in women.

Recently, one study used geese to detect hepatic steatosis and concluded that both fat percentages obtained by QCT and proton density fat fraction by MRI were highly correlated with chemical extraction²¹. However, there are still too few studies that directly use MRI, especially m-Dixon-Quant 3D scanning, to examine the changes in the L2–4 vertebral body and the corresponding diagnosis of OP. The m-Dixon-Quant sequence has a short scan time of only 51 seconds. During the period, the fat score map is intuitively displayed, and the lipid content is quantitatively and quickly quantified without recalculation. However, the m-Dixon-Quant sequence is not configured on all models with the latest development sequence, which is not fully used. We propose that FF% plays a direct role in MRI-based OP assessments and we strongly believe that our results can provide a potentially novel strategy for preventing and combating OP that extends beyond BMD observation. Finally, increasing evidence has indicated that BMD has its limitations in OP assessment, and whether BMD is of predictive value is still controversial. Given that MRI results are not only correlated with BMD values, but they also provide additional information for reference (MRI can provide the early detection of trabecular lesions, fractures, and deformities of the spine²²), CT and MRI are available tools that can potentially image and quantify the three-dimensional structure of trabecular bone¹⁶. A combination of these methods can further help to guide prevention and treatment strategies. Our results also suggest that FF%, together with QCT-acquired BMD, permit the structural and metabolic status of vertebrae.

Nevertheless, we noticed some studies that applied a similar approach to that employed in this investigation, but which obtained results that were inconsistent with ours. As we all know, the eating habits and exercise levels between Chinese race and Italian race are different. Thereby, bone density and vertebral fat content were different. A team from Italy used MR spectroscopy and diffusion-weighted MRI to observe heels in three groups of women (healthy controls, those with osteopenia, and those with OP), and claimed that marrow fat content did not significantly differ between groups, while the effective

internal magnetic field gradient (IMFG), a new MR parameter, held value in OP assessment²³. This inconsistency may be due to different patient profiles (especially related to patient sex) and to the different bone tissues evaluated in both studies.

There were also some limitations in this study. The study does not provide a quantitative analysis of OP, but also provide a differential diagnosis of benign compressive fractures of the spine. In this study, there is a high positive correlation between MRS and m-Dixon-Quant FF% and lipid-water ratio. With the appearance of bone marrow lesions, FF% has certain value for the benign and malignant diagnosis of fractures, which is basically consistent with previous studies²⁴⁻²⁶. The single nucleotide 1-H MRS has a statistically significant difference between MRS FF% and LWR in osteoporosis and tumor-induced benign and malignant compression fractures, which can effectively diagnose the benign and malignant compression fractures of the spine²⁷. It will be confirmed in the future study. In addition, the number of cases in this study was small, further increasing number of cases was needed to provide further diagnostic information for the diagnosis of osteoporosis.

Conclusions

In conclusion, our study indicates that MRI investigations (especially those that incorporate the FF% parameter) are useful in OP assessments. Further, parameters such as sex, age, and height are important factors for OP prediction and diagnosis.

Abbreviations

Osteoporosis (OP)

vertebral compression fracture (VCF)

Declarations

Ethics approval and consent to participate: The ethics committee of Honghui Hospital, Xi'an Jiaotong University College of Medicine approved the study.

Ethics, consent and permissions: This study was written informed consent from the patients.

Consent for publication: All contributing authors have agreed to submit this manuscript and all authors approved to publish this study.

We have obtained consent to publish from the participant to report individual patient data.

Availability of data and material: All data generated or analyzed during this study are included in this published article [and its supplementary information files].

Competing interests: The authors declare that they have no competing interests.

Funding: This study was funded by a grant from the Development Center for Medical Science and Technology National Natural Science Foundation of China (NSFC) (No. 81772357) and Natural Science Foundation for Shaanxi of China (No. 2017JM8152).

Authors' contributions: RC, XWM and YHJ designed and analyzed the experiment, and was a major contributor in writing the manuscript. DGH, XJC, MZ and DJH performed the experiment. All authors read and approved the final manuscript.

Acknowledgements: Not applicable.

References

1. Karahan AY, Kaya B, Kuran B, Altındag O, Yildirim P, Dogan SC, et al. Common Mistakes in the Dual-Energy X-ray Absorptiometry (DXA) in Turkey. A Retrospective Descriptive Multicenter Study. *Acta Medica*. 2017;59:117–23.
2. Angthong C, Angthong W, Harnroongroj T, Harnroongroj T. A comparison of survival rates for hip fracture patients with or without subsequent osteoporotic vertebral compression fractures. *Tohoku Journal of Experimental Medicine*. 2012;226:129.
3. Chao CT, Chiang CK, Huang JW, Chan DC, group COoGNiNTUHs. Effect of Frail Phenotype on Bone Mass and Vertebral Compression Fracture in Individuals Undergoing Dialysis. *J Am Geriatr Soc*. 2016;64:e19–21.
4. Oei L, Koromani F, Rivadeneira F, Zillikens MC, Oei EH. Quantitative imaging methods in osteoporosis. *Quant Imaging Med Surg*. 2016;6:680–98.
5. Licks R, Licks V, Ourique F, Radke BH, Fontanella V. Development of a prediction tool for low bone mass based on clinical data and periapical radiography. 2014.
6. Beaton DE, Dyer S, Jiang D, Sujic R, Slater M, Sale JEM, et al. Factors influencing the pharmacological management of osteoporosis after fragility fracture: results from the Ontario Osteoporosis Strategy's fracture clinic screening program. *Osteoporosis international: a journal established as result of cooperation between the European Foundation for Osteoporosis and the National Osteoporosis Foundation of the USA*. 2014;25:289–96.
7. Marshall D, Johnell O, Wedel H. Meta-analysis of how well measures of bone mineral density predict occurrence of osteoporotic fractures. *BMJ*. 1996;312:1254–9.
8. Wainwright SA, Marshall LM, Ensrud KE, Cauley JA, Black DM, Hillier TA, et al. Hip fracture in women without osteoporosis. *J Clin Endocrinol Metab*. 2005;90:2787–93.
9. Seeman E. Is a change in bone mineral density a sensitive and specific surrogate of anti-fracture efficacy? *Bone*. 2007;41:308–17.

10. Yamaga A, Taga M, Minaguchi H, Sato K. Changes in bone mass as determined by ultrasound and biochemical markers of bone turnover during pregnancy and puerperium: a longitudinal study. *J Clin Endocrinol Metab.* 1996;81:752–6.
11. Karchevsky M, Babb JS, Schweitzer ME. Can diffusion-weighted imaging be used to differentiate benign from pathologic fractures? A meta-analysis. *Skeletal Radiology.* 2008;37:791–5.
12. Gajewicz W, Papierz W, Szymczak W, Goraj B. The use of proton MRS in the differential diagnosis of brain tumors and tumor-like processes. *Med Sci Monit.* 2003;9:97–105.
13. O'Brien CM, Vargis E, Paria BC, Bennett KA, Mahadevan-Jansen A, Reese J. Raman spectroscopy provides a noninvasive approach for determining biochemical composition of the pregnant cervix in vivo. *Acta Paediatrica.* 2014;103:715–21.
14. Hollak C, Maas M, Akkerman E, Den HA, Aerts H. Dixon quantitative chemical shift imaging is a sensitive tool for the evaluation of bone marrow responses to individualized doses of enzyme supplementation therapy in type 1 Gaucher disease. *Blood Cells Molecules & Diseases.* 2001;27:1005–12.
15. Brasselet S, Ferrand P, Kress A, Wang X, Ranchon H, Gasecka A. Imaging Molecular Order in Cell Membranes by Polarization-Resolved Fluorescence Microscopy; 2012.
16. Ishida Y, Kawai S. [Diagnostic imaging in osteoporosis (CT and MRI)]. *Clin Calcium.* 2001;11:1561–7.
17. Hong J, Hipp JA, Mulkern RV, Jaramillo D, Snyder BD. Magnetic resonance imaging measurements of bone density and cross-sectional geometry. *Calcif Tissue Int.* 2000;66:74–8.
18. Ho KY, Hu HH, Keyak JH, Colletti PM, Powers CM. Measuring bone mineral density with fat-water MRI: comparison with computed tomography. *Journal of magnetic resonance imaging: JMRI.* 2013;37:237–42.
19. Lekadir K, Hoogendoorn C, Armitage P, Whitby E, King D, Dimitri P, et al. Estimation of trabecular bone parameters in children from multisequence MRI using texture-based regression. *Med Phys.* 2016;43:3071–9.
20. Baum T, Carballido-Gamio J, Huber MB, Müller D, Monetti R, Räth C, et al. Automated 3D trabecular bone structure analysis of the proximal femur—prediction of biomechanical strength by CT and DXA. *Osteoporosis International.* 2010;21:1553–64.
21. Kang GH, Cruite I, Shiehmorteza M, Wolfson T, Gamst AC, Hamilton G, et al. Reproducibility of MRI-determined proton density fat fraction across two different MR scanner platforms. *Journal of Magnetic Resonance Imaging.* 2011;34:928–34.

22. Becker C, Baltzer AW, Schneppenheim M, Becker A, Assheuer J, Merk HR, et al. [Experimental validation of DXA and MRI-based bone density measurement by ash-method]. *Zentralbl Chir.* 2001;126:402–6.
23. Rebuzzi M, Vinicola V, Taggi F, Sabatini U, Wehrli FW, Capuani S. Potential diagnostic role of the MRI-derived internal magnetic field gradient in calcaneus cancellous bone for evaluating postmenopausal osteoporosis at 3T. *Bone.* 2013;57:155–63.
24. Wang S, Radiology DO. Differential Diagnosis of Vertebral Compression Fractures Caused by Osteoporosis and Bone Metastases on MRI. *Practical Journal of Cancer.* 2014.
25. Cicala D,, Briganti F,, Casale L,, Rossi C,, Cagini L,, Cesarano E,, et al. Atraumatic vertebral compression fractures: differential diagnosis between benign osteoporotic and malignant fractures by MRI. *Musculoskeletal Surgery.* 2013;97:169–79.
26. Cho WI, Chang UK. Comparison of MR imaging and FDG-PET/CT in the differential diagnosis of benign and malignant vertebral compression fractures. *Journal of Neurosurgery Spine.* 2011;14:177.
27. Zhang L, Li S, Hao S, Yuan Z. Quantification of fat deposition in bone marrow in the lumbar vertebra by proton MRS and in-phase and out-of-phase MRI for the diagnosis of osteoporosis. *Journal of X-Ray Science and Technology.* 2016;24:257–66.

Figures

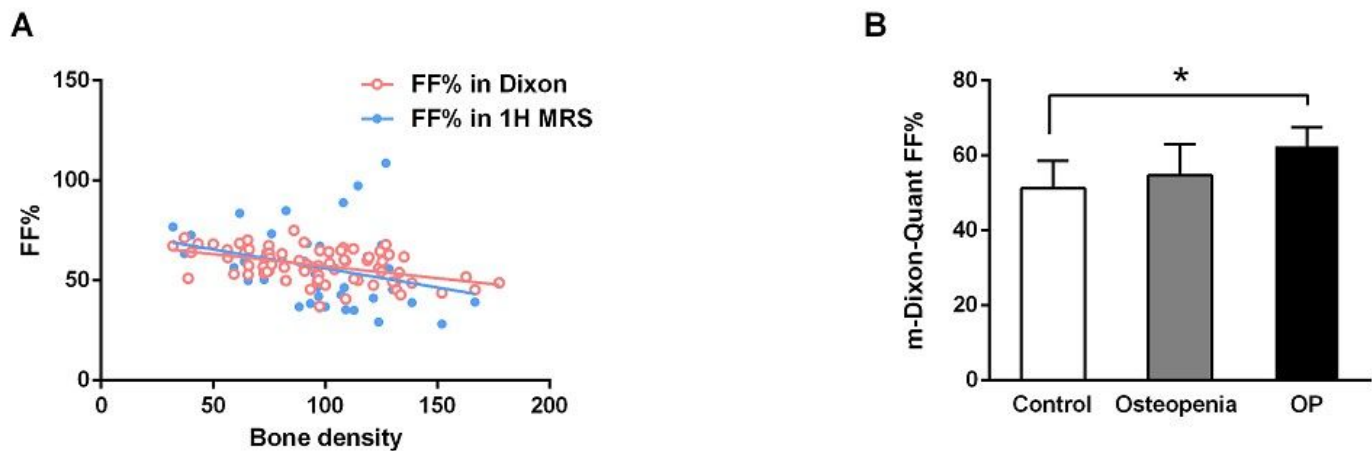


Figure 1

at fraction is negatively correlated with bone mineral density (BMD). (A) The percentage fat fraction (FF%) for both 1H MRS and m-Dixon-Quant imaging had a highly significantly negative correlation with the average bone density value. (B) The patients were divided into three groups: healthy controls, those with osteopenia, and those with osteoporosis (OP); the FF% value in the m-Dixon-Quant method was

significantly higher in the OP group when compared to controls. The bar presents the standard deviation; *P<0.05.

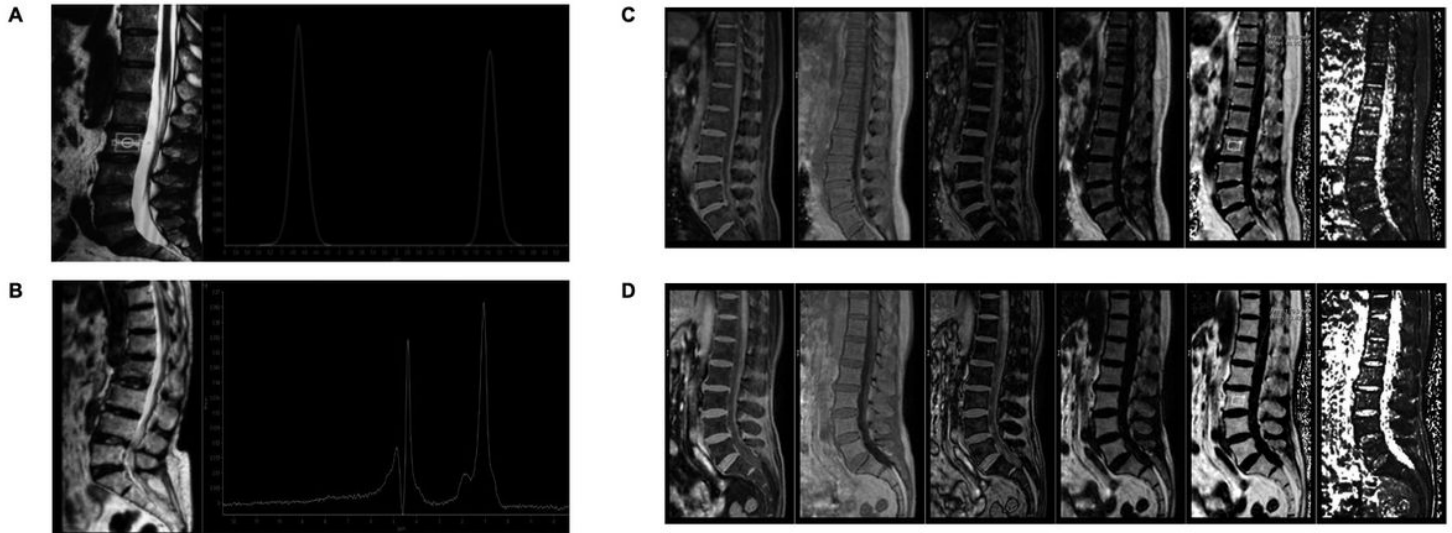


Figure 2

The 1H MRS and m-Dixon-Quant images of two individuals in different groups. The lipid peaks of the L2 vertebral body in the 1H MRS quantitative analysis of OP patients (B) were significantly increased compared to healthy controls (A). The signals of the L3 vertebral body in the m-Dixon-Quant analysis of healthy (C) and OP (D) cases.

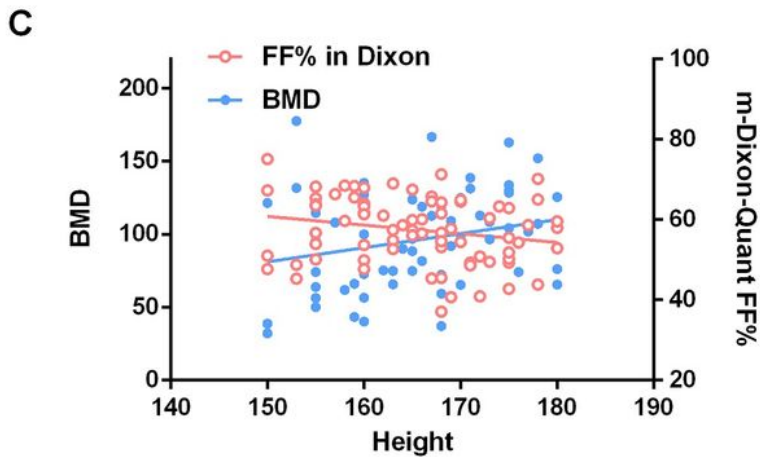
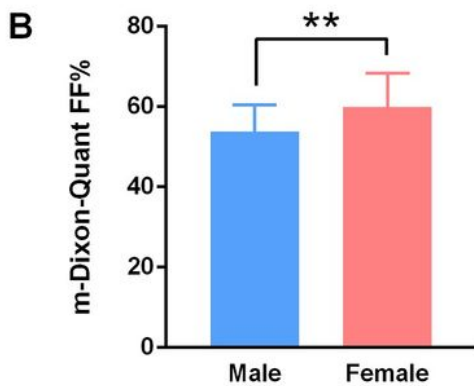
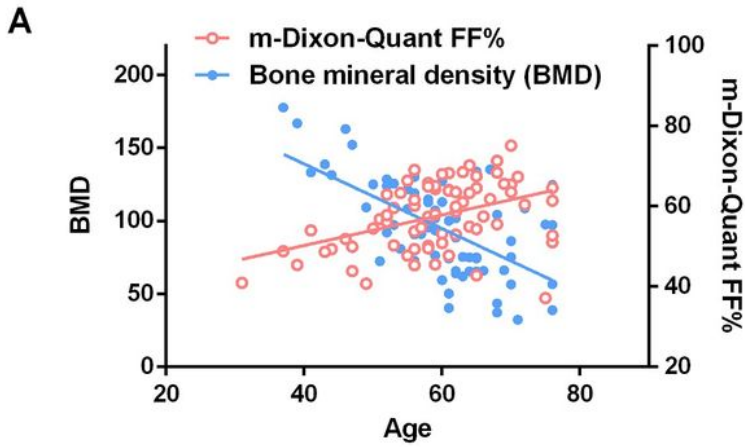


Figure 3

. Age, sex, and body height correlated with BMD and FF% changes. (A) Age largely determined BMD and FF levels (A). FF% in m-Dixon exhibited a positive correlation with age, while BMD showed a negative linear relationship. (B) Females had a higher FF% level compared to males. The bar presents the standard deviation; ** $P < 0.01$. (C) Body height was correlated with BMD, but not FF% ($P = 0.064$).